

**LIQUID PHASE REARRANGEMENT OF LONG STRAIGHT-CHAIN EPOXIDES  
OVER AMORPHOUS, MESOSTRUCTURED AND ZEOLITIC CATALYSTS**

David P. Serrano, Rafael van Grieken, Juan Antonio Melero\* and Alicia García  
Chemical and Environmental Engineering Group, ESCET, Rey Juan Carlos University,  
c/ Tulipán s/n, 28933, Móstoles, Spain.

Published on:

Applied Catalysis A: General, 269 (2004) 137-146

[doi:10.1016/j.apcata.2004.04.009](https://doi.org/10.1016/j.apcata.2004.04.009)

\*Corresponding author.

Tel: +34 91 488 70 87. Fax: +34 91 488 70 68

e-mail address: [j.melero@escet.urjc.es](mailto:j.melero@escet.urjc.es)

## **Abstract**

A variety of materials with different structural features and acid properties, including amorphous, mesostructured and zeolitic catalysts have been tested in the liquid-phase rearrangement of 1,2-epoxyoctane. The structure and acid strength of the catalysts influence strongly on the activity and product selectivity. The main rearrangement products are the aldehyde, allylic alcohols and diol. Acid sites in the amorphous materials show a poor catalytic activity. Al-TS-1 and Al-Ti-beta, zeolites with medium aluminium content, lead to significant activities and selectivities towards both the aldehyde and the octenols in comparison to those obtained with other zeolitic materials tested. Aluminium-containing mesostructured materials present much higher activities than amorphous and zeolitic catalysts. Al-MCM-41 synthesized by a sol-gel method at room temperature yielded selectivities to octaldehyde and octen-1ols of 40.6% and 44.7%, respectively with a high catalyst activity (TOF of ca. 30.5).

**Keywords:** epoxides, rearrangement, mesostructured materials, zeolites, Al-MCM-41.

## 1. Introduction

Hydroformylation of terminal alkenes, from his discovery by Roelen in 1938, has been used conventionally as one of the most versatile methods for the functionalization of terminal alkenes into carbonyl compounds. This process is based on the addition of carbon monoxide and hydrogen to the alkene double bond to yield aldehydes that can be subsequently hydrogenated to terminal alcohols or oxidized towards the corresponding carboxylic acids [1, 2]. However, this process has important drawbacks such as the high pressure, the use of high-cost homogeneous catalysts or the purification of the products. Moreover, the recovery of the rhodium-based catalysts is not an easy task. Other possible way for the synthesis of oxygenates from terminal olefinic compounds is the oxidative cleavage of the double bond to produce carbonyl groups. Several methods are available for this target, including the use of stoichiometric reagents such as potassium permanganate and ruthenium tetroxide, and complex catalytic systems with ozone and hydrogen peroxide [3, 4]. Nevertheless, this alternative involves a loss of the terminal carbon atom that makes inefficient the process from the point of view of atom economy.

Since both methods above mentioned for the preparation of carbonyl compounds show significant drawbacks, the development of an alternative process is an interesting goal. In this way, catalytic rearrangement of epoxides towards aldehydes has been shown as an attractive strategy of synthesis in Fine Chemistry. A number of studies on the catalytic rearrangement of epoxides have been reported, although most of them have dealt with homogeneous acid or base catalysts (e.g.  $\text{BF}_3$ ,  $\text{MgBr}_2$ ,  $\text{ZnCl}_2$ ,  $t\text{-BuOK}$  or lithium dialkylamides), whereas most of the substrates tested were highly reactive epoxides (cyclic-alkane, alkyl-aromatic and tertiary epoxides) [5, 6]. Acid-catalyzed epoxide rearrangement leads, usually to, ketones and aldehydes, whereas the base-catalyzed reaction of such derivatives yields allylic alcohols as main products [7].

The use of homogeneous catalysis presents numerous drawbacks: loss of the catalyst after reaction, corrosivity, toxicity and in most cases generation of contaminated streams. Accordingly, many efforts have been addressed to find out heterogeneous catalysts to overcome these problems. For this reason heterogeneous catalysts such as  $\text{SiO}_2$ ,  $\text{Al}_2\text{O}_3$ ,  $\text{ZrO}_2$ ,  $\text{TiO}_2$  or physical mixtures of them have been tested for epoxide rearrangement reactions [5]. The use of these conventional catalysts often results in the formation of aldol condensation products and mixtures of ketones and aldehydes as by-products. The voluminous molecules formed by aldol condensation are the first step in the formation of coke thus limiting the lifetime of these catalysts. Consequently, in the last years, zeolitic materials have attracted the attention because of their well defined pore system that may suppress the side reactions mentioned above [8-11].

A number of zeolites, including HZSM-5, H-Beta, Mordenite, Zeolite Y and X, have been tested in the rearrangement of aromatic or cyclic alkane epoxides as well as of epoxides with tertiary carbons linked to the oxirane ring. Thus, high selectivities to aldehydes have been obtained in the isomerization of styrene oxide and derivatives over various acid zeolites [12, 13]. Likewise, some works have been published on the use of zeolites as catalysts in the isomerization of small size aliphatic epoxides, such as propylene oxide and 2-methyl-2,3-epoxybutene, but in addition to the desired aldehyde different by-products were obtained [14, 15]. However, few results have been reported in regards to the rearrangement of long straight-chain 1,2-alkane epoxides. It must be pointed out that these kind of epoxides are low reactive substrates, hence the isomerization to the corresponding aldehyde involves stronger reaction conditions (higher temperature, catalyst loading and reaction time) and more active catalysts [16, 17]. An important amount of different monounsaturated terminal alcohols is also obtained using this kind of epoxides as substrate.

Linear aldehydes can be easily oxidised towards the corresponding carboxylic acid. The commercial value of linear carboxylic acids, and particularly of their salts and esters, is

mainly based on their synthetic utility. Much of them are used as intermediates for textile chemicals, dyes, drugs, plastics and agricultural chemicals. Both linear aldehydes and monounsaturated terminal alcohols can be also selectively hydrogenated to the corresponding linear alcohols. Industrially, the higher alcohols can be separated into plasticizers (C<sub>6</sub>-C<sub>11</sub>) and fatty alcohols (C<sub>12</sub>-C<sub>18</sub>), used for detergents. Moreover, aliphatic alcohols are used as solvents and diluents for paints, as intermediates in the manufacture of esters and in the preparation of a wide range of organic compounds.

These previous works prompted us to study the catalytic rearrangement of long straight-chain epoxides in liquid phase over different acid solid catalysts. The present paper describes the results obtained in the rearrangement of 1,2-epoxyoctane, chosen as a model epoxide, over different acid catalysts. We have checked the activity of several catalysts having a variety of acid properties and structural features, including different zeolites, amorphous and mesostructured materials.

## **2. Experimental**

### *2.1. Catalysts preparation*

#### *2.1.1. Amorphous materials*

An amorphous SiO<sub>2</sub>-TiO<sub>2</sub> xerogel was prepared through a two-step sol-gel method involving acid-hydrolysis of the precursors and basic gelation [18]. Alumina and alumina-silica were supplied by Merck and Südchemie, respectively.

### 2.1.2. Zeolitic materials

TS-1 zeolite was synthesized by hydrothermal crystallization of wetness impregnated SiO<sub>2</sub>-TiO<sub>2</sub> amorphous xerogels [18]. ZSM-5 zeolite was prepared by a conventional method from ethanol-containing gels [19]. Al-TS-1 and Al-Ti-beta zeolites were prepared by hydrothermal crystallization of wetness impregnated SiO<sub>2</sub>-TiO<sub>2</sub>-Al<sub>2</sub>O<sub>3</sub> xerogels [20, 21]. Al-beta zeolite, free of titanium, was prepared by hydrothermal synthesis in fluoride medium [22]. Two additional zinc-containing zeolites, CIT-6 and VPI-8 with BEA and VPI framework topology, respectively, were synthesized under hydrothermal treatment of clear hydrogels containing tetraethylammonium (TEA<sup>+</sup>), Li<sup>+</sup> and Zn<sup>2+</sup> cations [23]. Ultra-stable Y zeolite (USY) and mordenite were supplied by Grace and Zeolyst, respectively.

### 2.1.3. Mesostructured materials

Al-MCM-41 (SG) was synthesized by a sol-gel procedure at room temperature using aluminium isopropoxide as aluminium source [24]. Additionally, a different Al-MCM-41 material, denoted as Al-MCM-41 (HT), was synthesized by a conventional hydrothermal treatment in basic medium [25]. Al-SBA-15 was prepared by a sol-gel procedure using Pluronic 123 triblock copolymer (EO<sub>20</sub>-PO<sub>70</sub>-EO<sub>20</sub>; Aldrich) as polymeric template and aluminium isopropoxide as aluminium source [26].

## 2.2. Catalysts Characterization

All the catalytic samples were characterized by different techniques. Crystallinity of zeolitic samples and mesoscopic ordering of mesostructured materials were checked through X-Ray diffraction (XRD) patterns acquired with a Philips X'PERT MPD diffractometer using Cu K<sub>α</sub> radiation. Typically, the data were collected from 5 to 50° (2θ) for zeolitic samples and from

0.6 to 4° (2 $\theta$ ) for mesostructured materials with a resolution of 0.02°. Chemical analyses of the samples were performed by induced coupled plasma-atomic emission spectroscopy (ICP-AES) with a Varian VISTA-AX apparatus.

Nitrogen adsorption-desorption isotherms at 77 K of the calcined catalysts were obtained using a Micromeritics ASAP 2010 porosimeter. Previously, the samples were outgassed under vacuum at 200 °C for 5 h. The surface areas were determined according to the BET equation. Pore size distribution was obtained applying the BJH method to the adsorption branch of the isotherm. Cylindrical pore geometry was assumed for the calculations and the Jura-Harkins equation was used to determine the thickness of the adsorbed layer. The total pore volume was determined from the N<sub>2</sub> adsorption at p/p<sub>0</sub>=0.99. Micropore volume and external surface area of the catalysts were determined using the t-plot method. Morphology and size of the catalyst particles were obtained by scanning electron microscopy (SEM) with a JEOL JSM 6400 microscope.

The coordination of the aluminum atoms in the catalysts was checked by <sup>27</sup>Al-MAS-NMR spectra of the calcined samples. The spectra were recorded at 104.26 MHz in a VARIAN Infinity 400 spectrometer at spinning frequency of 4 KHz and intervals ranging from 5 to 30 s between successive accumulations were selected according to the structural nature of the sample. The external standard reference was [Al(H<sub>2</sub>O)<sub>6</sub><sup>+3</sup>] and all measurements were carried out at room temperature.

The acid properties of the catalysts were determined by ammonia temperature programmed desorption (TPD) in a Micromeritics 2910 (TPD/TPR) equipment. Previously, the samples were outgassed under an helium flow (50 Nml min<sup>-1</sup>) with a heating rate of 15 °C min<sup>-1</sup> up to 560 °C and kept at this temperature for 30 min. After cooling to 180 °C, an ammonia flow of 35 Nml min<sup>-1</sup> was passed through the sample for 30 min. The physisorbed ammonia was

removed by flowing helium at 180 °C for 90 min. The chemically adsorbed ammonia was determined by increasing the temperature up to 550 °C with a heating rate of 15 °C min<sup>-1</sup>, this temperature being kept for 30 min. The ammonia concentration in the effluent helium stream was measured through a thermal conductivity detector (TCD).

### 2.3. Catalytic experiments

The catalytic experiments were carried out in a 0.1 L stirred batch autoclave equipped with a temperature controller and a pressure gauge at 120°C for different reaction times under stirring (550 rpm) and autogenous pressure. This experimental set-up is also provided with a device to feed the epoxide into the teflon-lined reactor once the reaction temperature is reached. The solvent and the catalyst are initially placed in the teflon-lined reactor. The zero time of the reaction is considered when the temperature reaches the set-point value and the epoxide is loaded into the reactor. The composition of the reaction mixture was as follows: 1 g of 1,2-epoxyoctane, 20 g of toluene (water content less than 0.03 wt. %) and 40 or 200 mg of catalyst depending on its activity. Toluene was stored with A zeolite to minimize its water content. The catalyst, prior reaction, was dried overnight at 140 °C.

The reaction products were analyzed with a GC (VARIAN 3800) equipped with a capillary column (HP-FFAP) with dimensions 60 x 0.32 mm, using a flame ionization detector (FID). Identification of the different reaction products was also performed by mass spectrometry (VARIAN SATURN 2000) using standard compounds.



### 3. Results and discussion

#### 3.1 Catalysts properties

The main physicochemical and textural properties of the catalysts used in this work are summarized in Tables 1, 2 and 3 for the amorphous, zeolitic and mesostructured materials, respectively. The SiO<sub>2</sub>-TiO<sub>2</sub> xerogel synthesised through a two-step sol-gel method [18] is an amorphous material with high surface area characterised for possessing weak Lewis acid sites, not detected in the NH<sub>3</sub> TPD measurements. It shows a mesopore size distribution centered at 50 Å. Al<sub>2</sub>O<sub>3</sub> and SiO<sub>2</sub>-Al<sub>2</sub>O<sub>3</sub> samples are amorphous solid oxides with stronger Lewis acidity, although lower surface area compared to the SiO<sub>2</sub>-TiO<sub>2</sub> xerogel.

**Table 1.** Physicochemical properties of the amorphous catalysts.

Catalyst	Molar Ratio	Pore Diameter (Å)	Surface Area (m <sup>2</sup> g <sup>-1</sup> )	Pore Volume (cm <sup>3</sup> g <sup>-1</sup> ) <sup>a</sup>	Acidity (mmol g <sup>-1</sup> ) <sup>b</sup>	T max (°C) <sup>b</sup>
SiO <sub>2</sub> -TiO <sub>2</sub>	Si/Ti: 52	50	550	0.60	0.00	-
Al <sub>2</sub> O <sub>3</sub>	-	48	133	0.25	0.45	260
SiO <sub>2</sub> -Al <sub>2</sub> O <sub>3</sub>	Si/Al: 15	22-120	261	0.97	0.19	284

<sup>a</sup> Measured at P/P<sub>0</sub> = 0.99.

<sup>b</sup> Acid capacity and maximum desorption temperature in TPD measurements

Considering their pore diameters the microporous materials tested can be classified in medium and large pore size zeolites (Table 2). TS-1, ZSM-5 and Al-TS-1 are medium pore size zeolites with a pore diameter around 5.5 Å and a three-dimensional pore structure (MFI topology). Al-Ti-Beta and Al-Beta zeolites are large pore size zeolites with a three-dimensional BEA structure which possesses tortuous 12-membered ring channels along c-direction, having a cross section of 5.6 x 6.5 Å. These channels intersect with a set of straight 12-membered ring channels along a- an b- directions, having elliptical cross sections of 5.7 x 7.5 Å. Mordenite and

ultra-stable Y zeolite (USY) are microporous materials with a large pore size characterized by possessing a higher aluminium content compared to the other zeolitic materials. Mordenite presents a one-dimensional pore system with a pore diameter of 6.5 x 7.0 Å, whereas USY zeolite possesses a three-dimensional large pore system (7.4 Å) with supercages of 12 Å. CIT-6 and VPI-8 are both large pore crystalline zincosilicates, but with a different framework topology. CIT-6 presents BEA structure whereas VPI-8 is characterized by a one-dimensional pore system with a pore diameter of 5.9 Å. These two materials have been selected as catalyst in this work due to high activities and selectivities obtained in epoxide rearrangement processes with zinc chloride as homogeneous catalyst.

**Table 2.** Physicochemical properties of the zeolitic catalysts

Catalyst	Molar Ratio	Pore Diameter (Å)	Dc (µm) <sup>a</sup>	Surface Area (m <sup>2</sup> g <sup>-1</sup> )	Micropore Volume (cm <sup>3</sup> g <sup>-1</sup> ) <sup>b</sup>	Acidity (mmol g <sup>-1</sup> ) <sup>c</sup>	T max (°C) <sup>c</sup>
<b>Medium pore size</b>							
TS-1	Si/Ti: 40	5.4 x 5.4 5.1 x 5.7	0.5-0.7	525	0.18	0.00	-
ZSM-5	Si/Al: 30	5.4 x 5.4 5.1 x 5.7	5.0-7.0	495	0.17	0.43	358
Al-TS-1	Si/Al: 122 Si/Ti: 83	5.4 x 5.4 5.1 x 5.7	0.3-0.4	490	0.19	0.17	331
<b>Large pore size</b>							
Al-Ti-Beta	Si/Al: 41 Si/Ti: 57	5.6 x 6.5 5.7 x 7.5	0.2-0.3	552	0.23	0.47	319
Al-Beta	Si/Al: 57	5.6 x 6.5 5.7 x 7.5	1.0-1.2	567	0.26	0.20	285
Mordenite	Si/Al: 11	6.5 x 7.0	0.1-0.5	535	0.23	0.56	408
USY	Si/Al: 3.5	7.4	0.7-1.0	436	0.19	0.37	277
<b>Zn-containing zeolites</b>							
CIT-6	Si/Zn: 16	5.6 x 6.5 5.7 x 7.5	0.8-1.1	495	0.22	0.11	247
VPI-8	Si/Zn: 24	5.9 x 5.9	1.0-1.4	450	0.19	0.03	231

<sup>a</sup> Mean crystal size.

<sup>b</sup> Measured at P/P<sub>0</sub> = 0.99.

<sup>c</sup> Acid capacity and maximum desorption temperature in TPD measurements

From the NH<sub>3</sub> TPD results shown in Table 2, it can be seen that the acid strength in zeolites depend not only on the aluminium content but also on the catalysts topology. Mordenite present the highest strength of acid sites with a peak maxima of ammonia desorption placed at 408 °C. ZSM-5, Al-TS-1 and Al-Ti-beta exhibit sites of intermediate acid strength ( $T_{\max} = 358$ , 331 and 319 °C, respectively) compared to those of mordenite zeolite and the rest of catalysts. The aluminium-containing zeolitic materials were analyzed by <sup>27</sup>Al-MAS NMR in order to bear out the degree of aluminium incorporated into the zeolitic framework. All the samples show a distinct peak at 52 ppm corresponding to tetrahedral aluminium and a fairly small one placed at ~0 ppm assigned to the presence of low amounts of extraframework aluminium species with octahedral coordination. Zn-containing zeolites show acid sites with the lowest strength as concluded by the maximum desorption temperature in NH<sub>3</sub> TPD experiments of ca. 240 °C.

Al-MCM-41 (SG) and Al-MCM-41 (HT) are ordered mesoporous materials synthesized by two different methods, a sol-gel method at room temperature and a hydrothermal method in basic conditions, respectively. Although both samples have similar chemical composition with pore sizes above 2.0 nm, some significant differences are observed in their acid and textural properties.

**Table 3.** Physicochemical properties of the mesostructured catalysts.

Catalyst	Molar Ratio	Pore Diameter (Å)	Surface Area (m <sup>2</sup> g <sup>-1</sup> )	Pore Volume (cm <sup>3</sup> g <sup>-1</sup> ) <sup>a</sup>	Acidity (mmol g <sup>-1</sup> ) <sup>b</sup>	T max (°C) <sup>b</sup>
Al-SBA-15	Si/Al: 76	50	550	0.49	0.19	284
Al-MCM-41 (SG)	Si/Al: 39	21	1087	0.68	0.28	275
Al-MCM-41 (HT)	Si/Al: 36	23.5	1015	0.62	0.18	266

<sup>a</sup> Measured at p/p<sub>0</sub> = 0.99.

<sup>b</sup> Acid capacity and maximum desorption temperature in TPD measurements.

Figure 1 shows the nitrogen adsorption-desorption isotherms at 77 K and pore size distributions corresponding to Al-MCM-41 (SG) and Al-MCM-41 (HT) samples. The two isotherms in Figure 1.a are clearly of type IV, which are typical of mesoporous materials. The inflection points observed at relative pressures around 0.2 indicate that capillary condensation in mesopores occurs after the monolayer adsorption on the walls. For relative pressures above 0.5, the isotherms present an almost constant adsorption zone that, in the case of Al-MCM-41 (SG), suffers a significant increase at high relative pressures due to multilayer formation on the external surface of the particles. Significant differences can be appreciated in the pore size distributions of Figure 1.b. The Al-MCM-41 (SG) sample presents a wider pore size distribution and smaller pores with sizes in the micro-mesopore limit as compared to that observed for Al-MCM-41 (HT).

<sup>27</sup>Al MAS NMR spectra of both Al-MCM-41 samples after calcination show two clear peaks centred at ~4 ppm and ~50 ppm originated from octahedrally and tetrahedrally coordinated aluminium species, respectively. The relative proportion of octahedral to tetrahedral species is higher in Al-MCM-41 (HT) than in Al-MCM-41 (SG) and in both cases larger than that observed in zeolites. Al-SBA-15 is also a hexagonally ordered mesostructured material but with textural properties significantly different from Al-MCM-41. It exhibits a higher pore size, around 50 Å, a BET surface area appreciably lower, arising from a higher wall thickness, and the presence of complementary micropores located on the silica wall and providing connectivity between the mesostructured channels [27]. All the mesostructured materials possess acid sites with medium acid strength since their temperature maxima for ammonia desorption are placed around 280°C.

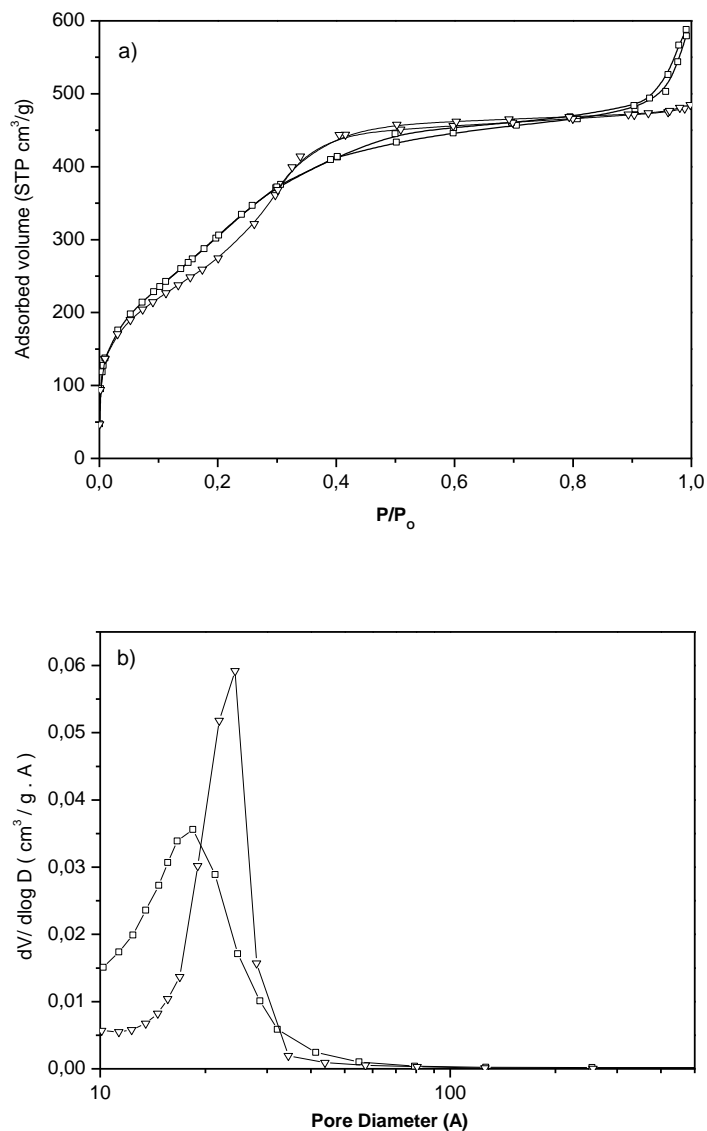


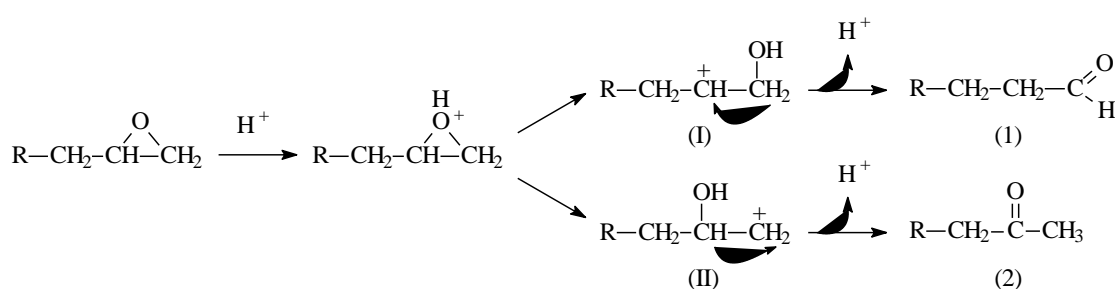
**Figure 1.** N<sub>2</sub> adsorption-desorption on the Al-MCM-41 materials: a) isotherms, b) pore size distributions (▽) Al-MCM-41 (SG) (◻) Al-MCM-41 (HT).

### 3.2. Catalytic epoxide rearrangement

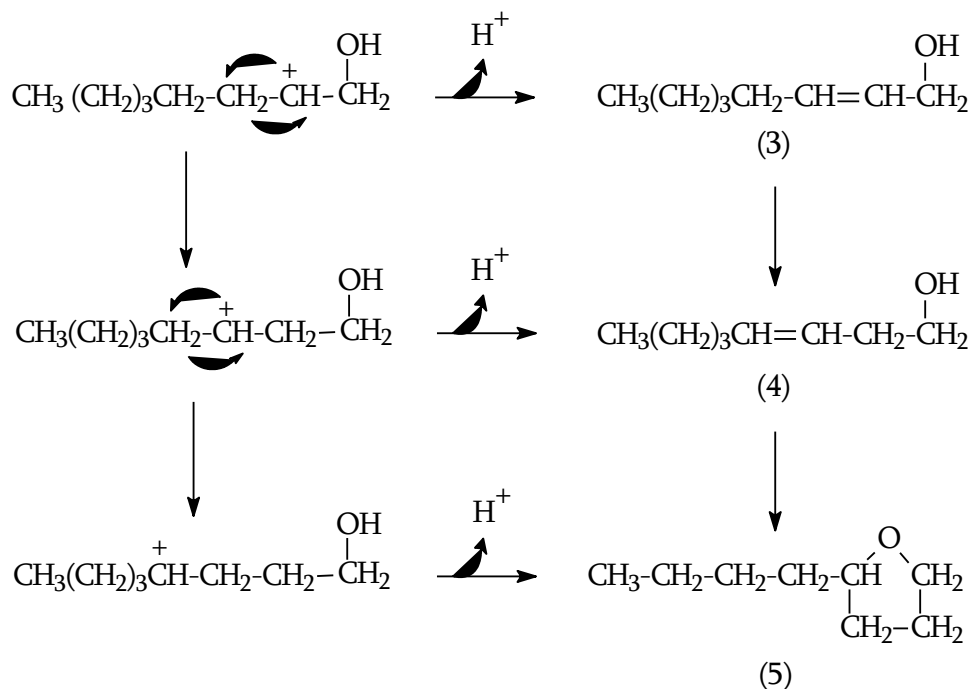
The results obtained over the different catalytic systems in the isomerization of 1,2-epoxyoctane in liquid phase are shown in Tables 5, 6 and 7 in terms of activity and product selectivity. Quantitative comparison of the catalysts have been addressed using the turnover

frequency (TOF) defined, as moles of reacted epoxide per mol of active site and hour. Since some epoxides may be isomerized thermally, a blank reaction in absence of catalyst was carried out that yielded a negligible conversion under the reaction conditions used in this work.

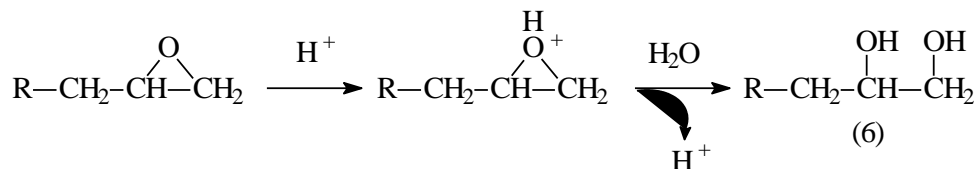
Most of the catalysts tested promote the isomerization of the epoxide towards the corresponding aldehyde (1) and ketone (2) through carbocation-mediated processes and subsequent 1,2-shift (Scheme 1). Additionally, other two important secondary reactions are also detected: the formation of different octenols coming from positive charge shift of one of the carbocations generated (Scheme 2) and diol generation by nucleophilic attack of water to the oxirane ring (Scheme 3). The formation of the different octenols (3 and 4) and of 1,4-epoxyoctane (5) is explained in terms of the different transpositions of the positive charge of the carbocation (Scheme 2). In all cases, the main product coming from these secondary reactions is 2-octen-1-ol (3) since the formation of allylic alcohols is always favoured. The appearance in the reaction product of relatively large amounts of diol indicates the presence of water probably contained in the solvent and/or originated from the dehydroxilation of silanols groups located on the surface of the catalysts.



**Scheme 1.** Carbocation formation in 1,2-epoxyoctane and subsequent 1,2-shift leading to carbonyl compounds: (1) Aldehyde and (2) Ketone.



**Scheme 2.** Transposition of the positive charge in 1,2-epoxyoctane leading to different octenols and 1,4-epoxyoctane: (3) 2-octen-1-ol, (4) 3-octen-1-ol and (5) 1,4-epoxyoctane.



**Scheme 3.** Nucleophilic attack by water of the oxirane ring in 1,2-epoxyoctane: (6) 1,2-octanediol.

Another type of product obtained in the rearrangement reaction of 1,2-epoxyoctane over heterogeneous catalysts is 2-oct-2-enyloxy-octan-1-ol, (7), whose presence has been confirmed by mass spectrometry indicating a  $\text{C}_{16}$  structure ( $m/e=256$ ). We postulate that this compound is formed by the nucleophilic attack of octenols to the epoxide as outlined in Scheme 4. With the purpose of confirming the formation mechanism of this compound we have performed an additional isomerization experiment using  $\text{ZnCl}_2$  as catalyst and in the presence of an initial amount of 2-octen-1-ol. The catalytic results shown in Table 4 evidence a significant





**Table 4.** 1,2-Epoxyoctane rearrangement over ZnCl<sub>2</sub> in presence and absence of 2-octen-1-ol

Run	Conversion (%)	Product distribution (mg)					
		1	3	4	6	2+5	7
1 <sup>a</sup>	98.3	379	111	0	45	122	240
2 <sup>b</sup>	98.7	461	1068	45	2	20	530

<sup>a</sup> Reaction conditions: 1,2-epoxyoctane: ca. 1 g; ZnCl<sub>2</sub>: 200 mg; time: 3 h.

<sup>b</sup> Reaction conditions: 1,2-epoxyoctane: ca. 1 g; 2-octen-1-ol: ca. 1 g; ZnCl<sub>2</sub>: 200 mg; time: 3 h.

The screening of the different catalytic systems has been carried out on the basis of their catalytic activity and selectivity towards valuable products such as aldehydes and octenols. Linear aldehydes can be conveniently transformed into linear carboxylic acids or terminal alcohols, important precursors in Organic Chemistry. Moreover, octenols can be also selectively hydrogenated to linear alcohols [28].

### 3.2.1. Epoxide rearrangement over amorphous catalyts.

Three different amorphous oxides (SiO<sub>2</sub>-TiO<sub>2</sub> xerogel, Al<sub>2</sub>O<sub>3</sub> and SiO<sub>2</sub>-Al<sub>2</sub>O<sub>3</sub>) have been tested in the liquid phase rearrangement of 1,2-epoxyoctane, obtaining the results shown in Table 5. The SiO<sub>2</sub>-TiO<sub>2</sub> xerogel evidences a very low activity, which correlates fairly well with its low acid strength shown by the ammonia TPD results. The activity obtained over Al<sub>2</sub>O<sub>3</sub> was not higher than that of the blank reaction whereas the SiO<sub>2</sub>-Al<sub>2</sub>O<sub>3</sub> catalyst presents a conversion somewhat higher than that obtained with the SiO<sub>2</sub>-TiO<sub>2</sub> xerogel. In terms of TOF both mixed oxides behave in a similar way, but the product distribution obtained is quite different. The SiO<sub>2</sub>-TiO<sub>2</sub> xerogel leads to a significant formation of diol (ca. 40.6%), probably related with the high content of hydroxyl groups present in this material, with low octaldehyde selectivity. However, the SiO<sub>2</sub>-Al<sub>2</sub>O<sub>3</sub> mixture yielded smaller diol selectivity (ca. 22.9%), but a higher amount of octaldehyde and 2-oct-2-enyloxy-octan-1-ol, although with a poor selectivity to

valuable products (octaldehyde+octen-1-ols: 55.6%). These catalytic results demonstrate that these materials do not catalyze effectively the isomerization of linear epoxides.

**Table 5.** 1,2-Epoxyoctane rearrangement over amorphous catalysts<sup>a</sup>

Catalyst	Conversion (%)	TOF <sup>b</sup>	Selectivity (%)				
			1	3+4	6	2+5	7
SiO <sub>2</sub> -TiO <sub>2</sub>	4.3	1.8 <sup>c</sup>	12.3	37.2	40.6	5.4	4.5
Al <sub>2</sub> O <sub>3</sub>	0.0	0.0	-	-	-	-	-
SiO <sub>2</sub> -Al <sub>2</sub> O <sub>3</sub>	14.3	1.9	33.4	22.2	22.9	3.7	17.8

<sup>a</sup> Reaction conditions: catalyst loading: 200 mg; time: 3 h.

<sup>b</sup> mol 1,2-epoxide converted/(mol Al·h) after 3 hours

<sup>c</sup> Activity per mol of Ti.

### 3.2.2. Epoxide rearrangement over zeolitic catalysts.

A number of works have been published regarding the use of zeolites as catalysts in epoxides isomerizations. The interest in such solids as catalysts in these kind of processes arises from their well defined pore system and high stability. Hölderich et al. have disclosed the rearrangement of 2-methyl-2,3-epoxybutene, 2-methylstyrene oxide and diisobutylene oxide to yield aldehydes in the presence of various zeolites of the pentasil type [29, 30]. Propanal can be prepared in gas phase from propylene oxide rearrangement over basic zeolites such as (Mg, Na)-Y with selectivities up to 88% [31]. Brunel et al. [16] have reported the 1,2-epoxyoctane rearrangement over zeolites HY, H-OFF and H-beta with selectivities towards octanal and allylic alcohol around 45% and 25%, respectively.

Taking these previous results as reference, we decided to test a variety of zeolitic materials with different framework topology and acid strength in the liquid phase rearrangement of 1,2-epoxyoctane. The results obtained have been summarized in Table 6. At the first attempt, we considered to study the catalytic performance of zeolites with medium pore size. TS-1, free

of strong Brönsted acid sites, was firstly tested. The activity results (TOF ca. 2.3) clearly indicate that the weak acid Lewis sites present in TS-1 does not promote properly the epoxide rearrangement. When a sample of ZSM-5 (Si/Al molar ratio of 30) was used as catalyst an increase in both TOF and conversion was observed, but no significant changes regarding the product distribution were detected.

Al-TS-1 with bifunctional properties due to the simultaneous presence of titanium and aluminium in the zeolite framework has been also tested. The results obtained suggest that acid sites in Al-TS-1 show a similar activity to those present in ZSM-5 sample. The higher conversion observed over ZSM-5 might be attributed to its higher aluminium content, although a greater value should be expected. This could be explained considering internal diffusional problems arising from the larger crystal size of ZSM-5 sample (5-7  $\mu\text{m}$ ) compared to that of Al-TS-1 (0.3-0.4  $\mu\text{m}$ ). From the results shown in Table 6, it can be observed that Al-TS-1 yields a higher amount of valuable products (octaldehyde+octen-1-ols: 74.5%) in comparison to the selectivities obtained with TS-1 and ZSM-5 zeolites.

Al-containing zeolites with larger pore size have been also investigated in order to promote the access of the substrate within the catalyst pores and avoid diffusional limitations. Al-Ti-Beta zeolite shows a similar activity per mol of acid site than Al-TS-1 and ZSM-5 but a higher epoxide conversion, probably due to its larger pore size. In contrast with the product distribution obtained with Al-TS-1, Al-Ti-Beta leads to an enhancement in the formation of 1,2-octanediol what decreases the selectivity towards valuable products (ca. 66.3%). Besides, another catalytic run has been carried out in presence of Al-beta zeolite synthesised by hydrothermal crystallization in a neutral medium (fluoride method). This material is characterised by possessing a high hydrophobic surface as a consequence of the low content of structural defects (silanols groups) in contrast with Beta zeolite samples synthesized under basic hydrothermal conditions. The low activity obtained with this material clearly indicates that the high

hydrophobic character of the sample hinder the accessibility of the polar substrate within the zeolite pores. Moreover, larger crystal size of the Al-beta sample compared to Al-Ti-beta could involve some diffusional problems that are avoided in the latter due to its smaller crystallites. Nevertheless, it is remarkable the high octen-1-ols selectivity obtained with this material (ca. 65.3%).

**Table 6.** 1,2-Epoxyoctane rearrangement over zeolitic and homogeneous catalysts<sup>a</sup>

Catalyst	Conversion (%)	TOF <sup>b</sup>	Selectivity (%)				
			1	3+4	6	2+5	7
<b>Medium pore size zeolites</b>							
TS-1	6.4	2.3 <sup>c</sup>	34.9	26.4	25.6	7.0	6.1
ZSM-5	24.5	6.2	33.6	31.2	20.8	9.2	5.2
Al-TS-1	13.5	5.0 <sup>d</sup>	25.3	49.2	15.1	7.7	2.7
<b>Large pore size zeolites</b>							
Al-Ti-Beta	36.2	6.4 <sup>d</sup>	29.3	37.0	23.8	6.7	3.2
Al-Beta	5.9	2.4	12.0	65.3	16.3	0.0	6.4
Mordenite	41.4	3.7	35.6	32.7	20.7	5.0	6.0
USY	10.3	0.4	18.2	46.7	29.2	4.3	1.6
<b>Zn-containing zeolites</b>							
CIT-6	10.7	1.3 <sup>e</sup>	3.9	77.6	17.1	0.0	1.4
VPI-8	0.0	0.0 <sup>e</sup>	0.0	0.0	0.0	0.0	0.0
<b>Homogeneous system<sup>f</sup></b>							
ZnCl <sub>2</sub>	46	2.4 <sup>e</sup>	59.8	5.9	0.9	5.8	27.6

<sup>a</sup> Reaction conditions: catalyst loading: 200 mg; time: 3 h.

<sup>b</sup> mol 1,2-epoxide converted/(mol Al·h) after 3 hours

<sup>c</sup> Activity per mol of Ti;

<sup>d</sup> Activity per mol of Al+Ti

<sup>e</sup> Activity per mol of Zn.

<sup>f</sup> Reaction conditions: catalyst loading: 200 mg; time: 1 h.

In order to gain more information about the catalytic performance of different zeolitic materials in this particular reaction, materials with a high aluminium content such as mordenite (Si/Al: 11; Dp: 6.5 x 7.0 Å) and ultra-stable Y zeolite (Si/Al: 3.5; Dp: 7.4 Å) have been also investigated. Under the conditions depicted in Table 6, mordenite sample shows the highest epoxide conversion with a value of around 41%. However, the activity per mol of active site obtained is low (TOF: 3.7) probably due to the one-dimensional pore system of this zeolite which could hinder the accessibility of reactants to the active sites. Ultra-stable Y zeolite, with a three-dimensional large pore system (7.4 Å), led to a low epoxide conversion and an almost negligible activity (10.3 % and 0.4, respectively). These results are quite different from those reported by Hölderich et al. in the rearrangement of  $\alpha$ -pinene oxide over USY zeolite [8]. However our catalytic results illustrate clearly the lower reactivity of long-straight chain epoxides. The product distribution obtained when mordenite is used as catalyst is similar to the results shown by ZSM-5 sample, whereas USY zeolite leads to the highest diol selectivity (ca 29.3%) and a high amount of octen-1-ols (ca. 46.7%).

Finally, since zinc chlorides are known to be effective homogeneous catalysts in epoxides rearrangement [5], we have considered the use of zinc-containing zeolites in this kind of process. Thus, two zinc-containing zeolites with BEA and VPI structure, characterised for possessing Lewis acid sites were used as catalysts and compared with ZnCl<sub>2</sub>. The catalytic results obtained over VPI-8 zincosilicate were disappointing, since it showed a negligible activity. In contrast, the CIT-6 zincosilicate presented an epoxide conversion similar to that of Al-TS-1 zeolite but with a lower activity per mol of active site. The product distribution obtained over CIT-6 is interesting due to the high octen-1-ols selectivity obtained (ca. 77.6%). It is noteworthy that the use of the homogeneous catalytic system, ZnCl<sub>2</sub>, leads to a low activity per mol of active site (TOF: ca. 2.4). Likewise, this system yielded an octaldehyde selectivity of 59.8 %, higher than that obtained with the heterogeneous catalytic system based on Al-

containing zeolites, but with lower octen-1-ols selectivity. Note that the formation of the bulky (7) compound is clearly enhanced as a consequence of the absence of sterical restrictions.

In conclusion, Al-containing zeolitic materials with a medium aluminium content seems to be active in the rearrangement of 1,2-epoxyoctane in liquid phase towards the corresponding aldehyde and octenols although a high amount of undesirable diol is formed. Nevertheless, the extension of the reaction seems to be dramatically influenced by the limitations of the pore and crystal size. Note that all the zeolitic materials catalyses the formation of the bulky 2-oct-2-enyloxy-octan-1-ol compound (scheme 4) in spite of their limited pore size although in less extent than in  $\text{SiO}_2\text{-Al}_2\text{O}_3$  catalyst and homogeneous system. Probably, the external acid sites of these zeolitic materials are acidic enough to catalyse the formation of this compound.

### *3.2.3. Epoxide rearrangement over Al-containing mesostructured catalysts.*

The discovery of mesoporous molecular sieves of the M41S family [32] opened new possibilities for the preparation of catalysts with uniform pores in the mesoporous range, easily accessible for bulky molecules and, thus, without limitations typical of microporous materials. The possibility of incorporating aluminium into the silica walls turned these materials into solids with acid sites of medium strength, with potential applications as acid catalysts in different reactions (cracking, hydrocracking, etc.) [33]. The presence of both Brönsted and Lewis acid sites on aluminium-containing mesostructured materials prompted us to check this kind of materials in the liquid phase isomerization of 1,2-epoxyoctane, with the purpose of studying the influence of catalytic systems with pore sizes and acidity very different from those present in zeolitic materials. Moreover, up to the best of our knowledge, the work here reported is the first using aluminium-containing mesostructured materials as catalysts for long-straight chain epoxide rearrangement.

Three catalytic experiments were carried using aluminium-containing SBA-15 and MCM-41 materials synthesised in our laboratory. Preliminary experiments with these materials (not shown) yielded a sharp enhancement of catalytic activities as compared with the catalysts mentioned above. Therefore, a lower catalyst loading was used in order to obtain comparative epoxide conversions (ca. 40 mg).

We found that all mesoporous materials tested present much higher activities per active site in comparison to those obtained with zeolitic materials. These results probably arise from the larger pores of mesostructured materials that avoid diffusional problems present in zeolitic catalysts. Al-SBA-15 shows an activity lower than Al-MCM-41 samples in spite of the similar strength of the acid sites obtained by TPD measurements. This fact may be assigned to the presence of an important amount of active sites located in the microporosity of SBA-15 materials, which hinders the accessibility of the substrate.

Al-MCM-41 (SG), synthesized by a sol-gel method at room temperature, yields selectivities to octaldehyde and octen-1-ols of 40.6% and 44.7%, respectively, which means an overall selectivity towards valuable products near 85 %. Moreover, its catalyst activity is 10-20 times higher than those obtained with zeolites (TOF: ca. 68). Surprisingly, the catalytic results obtained with Al-MCM-41 (HT) are very different to that showed by Al-MCM41 (SG) in terms of product distribution. The use of Al-MCM-41 (HT) as catalyst on 1,2-epoxyoctane rearrangement enhances the formation of a high amount of 1,2-octanediol (45.1%) with a poor yield to valuable products (octanal+octen-1-ols selectivity: ca. 44.6%). The treatment of this catalyst with trimethylsilane may result in an improvement of the catalytic performance towards the formation of valuable products.

Such different results might be attributed to the different properties of the catalysts synthesised by the sol-gel method such as lower mesostructured ordering, wide pore size

distribution, better accessibility of acid centers (see TPD measurements in Table 3), higher adsorption capacity of molecules and lower content of aluminium extraframework species that may affect the catalytic behaviour. In line with our catalytic results some researchers have postulated that less ordered mesoporous materials are generally more catalytic active than those having ordered hexagonal pores [34]. This enhancement of the activity may result from the presence of interconnected mesopores that would allow easier access of substrate to the active sites.

**Table 7.** 1,2-Epoxyoctane rearrangement over mesoporous materials<sup>a</sup>

Catalyst	Conversion (%)	TOF <sup>b</sup>	Selectivity (%)				
			1	3+4	6	2+5	7
Al-SBA-15	5.9	29.2	29.6	48.2	9.4	11.4	1.4
Al-MCM-41 (SG)	30.5	67.9	40.6	44.7	7.9	5.7	1.1
Al-MCM-41 (HT)	29.0	56.6	36.1	8.5	45.1	5.0	5.3

<sup>a</sup> Reaction conditions: catalyst loading: 40 mg; time: 2 h.

<sup>b</sup> mol 1,2-epoxide converted/(mol Al·h) after 2 hours.

Finally, Figure 2 summarises the activity of the different catalytic systems in terms of TOF as a function of the pore diameter. Amorphous SiO<sub>2</sub>-TiO<sub>2</sub> material shows a poor catalytic activity, which correlates with the low acid strength of their acid sites. Amorphous SiO<sub>2</sub>-Al<sub>2</sub>O<sub>3</sub> material yields a low activity in spite of having a similar acid strength than that shown by mesostructured materials. This fact may be attributed to the lower accessibility of acid centers clearly evidenced in TPD measurements. In general zeolitic materials suffer from diffusional problems, which hinder the access of the linear epoxide to the active sites. Mesostructured Al-MCM-41 materials combine an appropriate pore size as well as a suitable accessibility and acid strength of their active sites that allow the highest activity. In contrast, Al-SBA-15 in spite of having acid sites of similar strength to those shown by Al-MCM-41 materials and even higher



pore sizes yielded a low activity. This fact is probably assigned to a lower accessibility of the active sites in this material, as they may be located in the complementary micropores existing in the SBA-15 silica walls. Note that TOF values in mesostructured materials are about one order of magnitude higher than in zeolites. These catalytic results show that both a medium acid strength and high accessibility of acid sites are essential factors to obtain high activity in the rearrangement of linear epoxides.

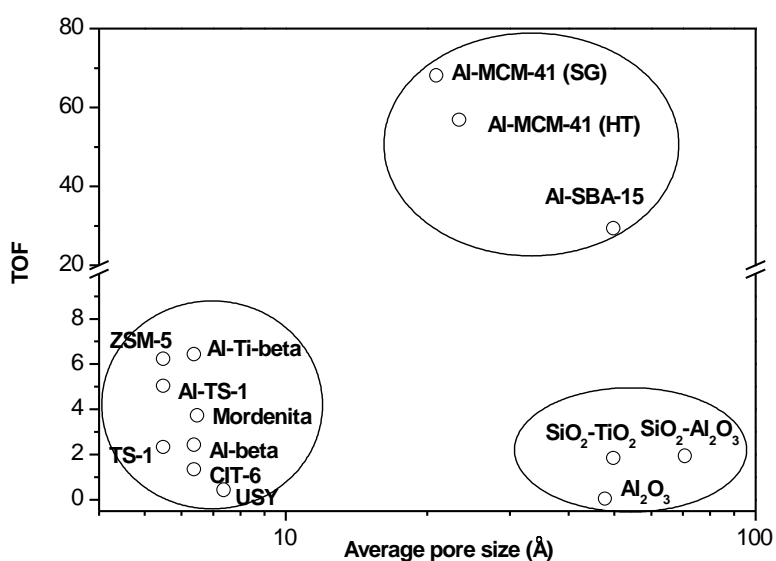


**Figure 2.** Activity of the different catalysts plotted versus the average pore size

From all the results obtained, it can be concluded that Al-MCM41 (SG) materials present the best catalytic performance, regarding to both activity and valuable product distribution. This kind of materials catalyzes selectively the isomerization of 1,2-epoxyoctane leading to a mixture of the corresponding aldehyde and octen-1-ols.

#### 4. Conclusions

The activity and selectivity of several catalysts with a wide range of acid properties and structural features, including amorphous oxides, zeolites and mesostructured materials, have been checked in the liquid phase rearrangement of 1,2-epoxyoctane. Amorphous  $\text{SiO}_2\text{-Al}_2\text{O}_3$  material shows a poor catalytic activity which correlates with the low accessibility of acid centers. Among zeolites, mordenite leads to the highest epoxide conversion because of its high aluminium content, but the activity per mol of active site is very low, probably because of diffusional problems arising from the one-dimensional pore system of this zeolite. ZSM-5, Al-TS-1 and Al-Ti-beta, which exhibit sites of intermediate acid strength, present a similar catalytic activity, although Al-Ti-beta leads to a higher epoxide conversion due to its larger pore size. Zn-containing zeolites, in particular CIT-6, catalyses selectively the formation of octen-1-ols. The extension of the reaction over zeolitic materials seems to be influenced by limitations of both pore and the crystal size of the catalysts. All mesoporous materials tested present much higher activities per active site in comparison to those obtained with zeolitic materials, probably arising from its larger pore sizes. The best catalytic activity has been obtained with Al-MCM-41 mesostructured materials presenting acid sites of medium acid strength.

Regarding to the product distribution, most of the catalysts tested promote the isomerization of the epoxide towards the aldehyde and octen-1-ols through carbocation-mediated processes. These octen-1-ols must be considered as interesting products as they can be hydrogenated to terminal alcohols with a high added-value. Additionally, the absence of water is a necessary requirement in order to avoid the nucleophilic attack of the oxirane ring with the consequent formation of diol. Amorphous materials present poor selectivities to valuable products with values close to 50%, whereas zeolites enhance the formation of the aldehyde and/or octen-1-ols with selectivities to octanal+octen-1-ols higher than 60%. Al-TS-1 zeolite yields a high selectivity towards valuable products reaching a value of almost 75 %. On the

other hand, Al-beta and CIT-6 lead mainly to octen-1-ols with values over 65%. The homogeneous catalytic system leads to the formation of a high amount of aldehyde (59.8 % selectivity), but with a low octen-1-ols selectivity. Al-MCM-41 synthesized by a sol-gel method yield high selectivities to valuable products. In particular, sol-gel Al-MCM-41 catalyzes selectively the isomerization of 1,2-epoxyoctane with selectivities to octaldehyde and octen-1-ols of 40.6% and 44.7%, respectively. The high formation of octenols (in particular the allylic alcohol) could result from the medium acid strength of these materials.

In summary, Al-MCM-41, prepared by the sol-gel method, is a material with remarkable catalytic properties for the isomerization of long-straight epoxides in liquid phase. It presents a high surface area and, although its acidity is weaker than that of zeolites, the access of the epoxide molecules to the active sites is not hindered as in the latter.

### **Acknowledgements**

We gratefully acknowledge the financial support of this work by "Consejería de Educación de la Comunidad de Madrid" (Contrato Programa Grupos Estratégicos de Investigación).

## References

1. M. Lenarda, L. Storaro, G. Renzo, *J. Mol. Catal.* 111 (1996) 203.
2. T. Onoda, *Chemtech*. September (1993) 34.
3. A. Johnstone, P.J. Middleton, W.R. Sanderson, WO Patent 95 100 243 (1995), to Solvay Interlox Limited.
4. S. Warwel, M. Klass, US Patent 5 321 158 (1994), to Solvay Interlox GmbH.
5. K. Arata, K. Tanabe, *Catal. Rev.-Sci. Eng.* 25 (1983) 365.
6. I. Erden, *Compr. Heterocycl. Chem.* II (1996) 97.
7. J. Marc, *Advanced Organic Chemistry*, John Wiley Ed., New York, 1985.
8. W.F. Hölderich, J. Röseler, G. Heitmann, A.T. Liebens, *Catal. Today* 37 (1997) 353.
9. J.A. Elings, H.E.B. Lempers, R.A. Sheldon, *Stud. Surf. Sci. Catal.* 105 (1997) 1165.
10. R.A. Sheldon, H. van Bekkum (Ed.), *Fine Chemicals through Heterogeneous Catalysis*, Wiley-VCH, Weinheim, 2001, p. 217.
11. R. Dimitrova, V. Minkov, N. Micheva, *Appl. Catal. A* 145 (1996) 49.
12. E. Ruiz-Hitzky, B. Casal, *J. Catal.* 92 (1985) 291.
13. M. Chamoumi, D. Brunel, P. Geneste, P. Moreaus, J. Solofo, *Stud. Surf. Sci. Catal.* 59 (1991) 573.
14. M. J. Faraj, US Patent 5 312 995 (1993), to Arco Chemical Technology.
15. W.F. Hölderich, N. Götz, L. Hupfer, H. Lermer, US Patent 4 980 511 (1987), to Basf AG.
16. D. Brunel, M. Chamoumi, P. Geneste, P. Moreau, *J. Mol. Catal.* 79 (1993) 297.
17. G.D. Yadav, D.V. Satoskar, *J. Chem. Tech. Biotechnol.* 69 (1997) 438
18. M.A. Uguina, G. Ovejero, R. van Grieken, D.P. Serrano, M. Camacho, *J. Chem. Soc., Chem. Commun.* (1994) 27.
19. R.J. Argauer, G.R. Landolt, US Patent 3 702 886 (1972), to Mobil Co.

20. G. Ovejero, R. van Grieken, M.A. Uguina, D.P. Serrano, J.A. Melero, *Catal. Lett.* 41 (1996) 69.
21. D.P. Serrano, M.A. Uguina, G. Ovejero, R. van Grieken, M. Camacho and J.A. Melero, *J. Mater. Chem.* 9 (1999) 2899.
22. M.A. Cambor, A. Corma, S. Valencia, *J. Mater. Chem.* 8 (1998) 2137.
23. D.P. Serrano, R. van Grieken, M.E. Davis, J.A. Melero, A. Garcia, G. Morales, *Chem Eur. J.* 8 (2002) 5153.
24. J. Aguado, D.P. Serrano, J.M. Escola, *Microporous Mesoporous Mater.* 34 (2000) 43.
25. W. Lin, Q. Cai, W. Pang, Y. Yue, B. Zon, *Microporous Mesoporous Mater.* 33 (1999) 217.
26. J. Aguado, D.P. Serrano, R. van Grieken, J.M. Escola, E. Garagorri, *Stud. Surf. Sci. Catal.* 135 (2001) 3915.
27. M. Kruk, M. Jaroniec, *Chem. Mater.* 12 (2000) 1961; R. Ryoo, C.H. Ko, M. Kruk, V. Antochshuk, M. Jaroniec, *J. Phys. Chem. B.* 104 (2000) 11465; C.G. Göltner, B. Smarsly, B. Berton, M. Antonietti, *Chem. Mater.* 13 (2001) 1617; R. van Grieken, G. Calleja, G.D. Stucky, J. A. Melero, R.A. Garcia, J. Iglesias, *Langmuir* 19 (2003) 3966.
28. G. Szöllösi, I. Kun, B. Török, M. Bartók, *Stud. Surf. Sci. Catal.* 125 (1999) 539.
29. W.F. Hölderich, N. Goetz, L. Hupfer, H. Lermer, US Patent 4 980 511 (1987), to Basf AG.
30. W.F. Hölderich, W.D. Mross, F. Merger, F. Fouquet, US Patent 4 929 765 (1984), to Basf AG.
31. M.K. Faraj, US Patent 5 312 995 (1993), to Arco Chemical Technology.
32. C.T. Kresge, M.E. Leonowicz, W.J. Roth, J.C. Vartulli, J.S. Beck, *Nature* 359 (1992) 710.
33. A. Corma, *Chem. Rev.* (1997) 273.
34. D.W. Park, S.D. Choi, S.J. Choi, C.Y. Lee, G.J. Kim, *Catal. Lett.* 78 (2002) 145.